QCD SUM RULES: FROM QUANTUM-MECHANICAL OSCILLATOR TO PION STRUCTURE IN QCD*

A.P. Bakulev

Bogoliubov Laboratory of Theoretical Physics, JINR
141980 Dubna, Moscow Region, Russia
bakulev@theor.jinr.ru

(Received October 3, 2006)

We illustrate the general scheme of the Sum Rule (SR) method using 2D Quantum Harmonic Oscillator (2DQHO) as a toy model. We introduce correlator, related to Green function of 2DQHO, and describe the property of Asymptotic Freedom for 2DQHO. We explain how the duality conception allows one to describe excited states. Finally we present numerical results and extract some lessons to learn from our exposition. Then we switch to the QCD and show that QCD SRs supply us the method to study hadrons in non-perturbative QCD.

PACS numbers: 11.55.Hx, 12.38.Lg

1. Quantum-mechanical toy model

Two-dimensional oscillator with potential $V(\vec{r}) = m\omega^2 r^2/2$ is the simplest system with confinement. We select this particular case $D = 2$ because all formulas greatly simplify, for example, energy levels and wave function values in the origin are

$$E_n = (2n+1)\omega\,; \qquad |\psi_n(0)|^2 = \frac{m\omega}{\pi}\,. \tag{1.1}$$

We will consider the regular quasi-perturbative method of Sum Rules (SR) to determine energy E_0 and $|\psi_0(0)|^2$ of the ground state. We follow here partially the lectures [1].

The general scheme of the SR method [2] can be easily understood on the example of a correlator $M(\mu)$, which has the spectral expansion:

$$M^{\rm spec}(\mu) = |\psi_0(0)|^2\, e^{-E_0/\mu} + \text{“higher states”}\,. \tag{1.2}$$

* Presented at the XLVI Cracow School of Theoretical Physics, Zakopane, Poland May 27–June 5, 2006.

Suppose that we can construct the perturbative expansion of this correlator:

$$M^{\rm pert}(\mu) = M_0(\mu) + \sum_{n\geq 1} C_{2n}\frac{\omega^{2n}}{\mu^{2n}}\,, \tag{1.3}$$

where $M_0(\mu)$ corresponds to "free movement" and has the spectral representation:

$$M_0(\mu) = \int\limits_0^\infty \rho_0(E)\, e^{-E/\mu}\, dE\,. \tag{1.4}$$

The sum rule — it is simply

$$M^{\rm spec}(\mu) = M^{\rm pert}(\mu)\,.$$

Usually it appears that higher state contributions can be well approximated by "free states" outside interval $(0, S_0)$. As a result we have SR in the form:

$$|\psi_0(0)|^2\, e^{-E_0/\mu} = \int\limits_0^{S_0} \rho_0(s)\, e^{-s/\mu}\, ds + C_2\frac{\omega^2}{\mu^2} + C_4\frac{\omega^4}{\mu^4} + \ldots \tag{1.5}$$

Our aim: to determine $|\psi_0(0)|^2$ and E_0 from this SR by calculating spectral density $\rho_0(E)$ of "free particle" and coefficients C_{2n} by demanding stability of this SR in variable $\mu \in [\mu_{\mathbf{L}}, \mu_{\mathbf{U}}]$ with appropriate value of S_0.

In order to select $M(\mu)$ with these properties for our 2DQHO let us consider 2-time Green function[1]

$$G(0,0|\vec{x},t) = \sum_{k\geq 0} \psi_k^*(\vec{x})\psi_k(0)e^{-iE_k t}\,, \tag{1.6}$$

which is the probability amplitude for the transition $(x=0, t=0) \to (\vec{x}, t)$. To get $M(\mu)$ we put $x=0$, $t = 1/i\mu$

$$M(\mu) = G(0,0|0,1/i\mu) = \sum_{k\geq 0} \left|\psi_k(0)\right|^2 e^{-E_k/\mu} = M^{\rm spec}(\mu)\,. \tag{1.7}$$

In our case $\left|\psi_k(0)\right|^2 = m\omega/\pi$, so we have the *exact result* for our $M(\mu)$:

$$M(\mu) = \frac{m\omega}{2\pi\, \sinh\left(\omega/\mu\right)}\,. \tag{1.8}$$

[1] Due to the fact that $\psi_k(0) = 0$ for all states with $L \geq 1$ only S-states contribute to this sum.

How fast is convergence of spectral expansion (1.7) for $M(\mu)$? Let us estimate it for $\mu = \omega$. Exact result (1.8) gives us $M(\omega) = (m\omega/2\pi) \cdot 0.851$, whereas numerically

$$M^{\rm spec}(\omega) = \frac{m\omega}{2\pi}\ (0.736 + 0.100 + 0.013 + 0.002 + \dots)\ .$$

Ground state contributes 86%, first excitation — 12%, while the second — only 1.5%.

Now we turn to the perturbative expansion of $M(\mu)$ in powers of (ω/μ):

$$M^{\rm pert}(\mu) = \frac{m\mu}{2\pi}\left(1 - \frac{\omega^2}{6\mu^2} + \frac{7}{360}\frac{\omega^4}{\mu^4} - \frac{31}{15120}\frac{\omega^6}{\mu^6} + \dots\right), \qquad (1.9)$$

Here $m\mu/2\pi$ corresponds to the Green function of free particle:

$$M^{\rm free}(\mu) = \frac{m\mu}{2\pi}\,. \qquad (1.10)$$

Numerically at $\mu = \omega$ we have

$$M^{\rm pert}(\omega) = \frac{m\omega}{2\pi}\ (1 - 0.167 + 0.019 - 0.002 + \dots)\ .$$

First correction specifies free result by 17%, while the second by 3%. This perturbative expansion can be rewritten

$$\frac{M(\mu) - M_0(\mu)}{M_0(\mu)} = -\frac{\omega^2}{6\mu^2} + \frac{7}{360}\frac{\omega^4}{\mu^4} - \frac{31}{15120}\frac{\omega^6}{\mu^6} + \dots\,, \qquad (1.11)$$

that means *Asymptotic Freedom*: $M(\mu)$ behaves like $M_0(\mu)$ at large $\mu \gg \omega$! And it is violated by power corrections of the type $\left(\omega^2/\mu^2\right)^n$.

We see in Fig. 1 that for large μ asymptotic freedom works well: $M(\mu) \simeq M_0(\mu)$, but we need more and more resonances to saturate $M(\mu)$. For small μ in spectral part survives only ground state $|\psi_0|^2 e^{-E_0/\mu}$, but the perturbation expansion breaks down. In order to model higher resonances let us consider the spectral representation of our correlator $M(\mu)$:

$$M^{\rm spec}(\mu) = \sum_{k\geq 0}\frac{m\omega}{\pi}\,e^{-E_k/\mu} \equiv \int\limits_0^\infty \rho^{\rm osc}(E)\,e^{-E/\mu}\,dE\,. \qquad (1.12)$$

Here the spectral density is just the sum of δ-functions:

$$\rho^{\rm osc}(E) = \sum_{k\geq 0}\frac{m\omega}{\pi}\,\delta(E - E_k)\,. \qquad (1.13)$$

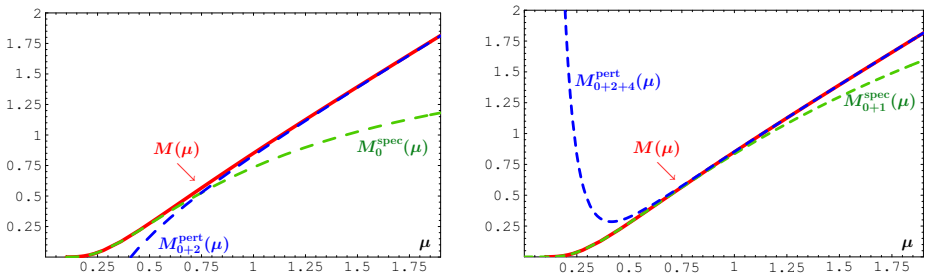


Fig. 1. In both panels the exact correlator, $M(\mu)$, (1.8), is shown by the solid line. Left panel displays also the ground state contribution only, $M_0^{\rm spec}(\mu)$ (the upper dashed line) and $M_0(\mu)+O(\omega^2/\mu^2)$ (the lower dashed line). In the right panel the ground + 1-st excited state contribution only, $M_{0+1}^{\rm spec}(\mu)$, is shown by the dashed line to the right, whereas $M_0(\mu)+O(\omega^4/\mu^4)$ — by the dashed line to the left.

Analogously we have integral representation for free correlator:

$$M_0(\mu)=\frac{m\mu}{2\pi}\equiv\int\limits_0^\infty\rho_0(E)\,e^{-E/\mu}\,dE\,, \tag{1.14}$$

where $\rho_0(E)=m/(2\pi)$. Asymptotic freedom dictates *global duality* of these two densities (term "global" is related with integration over the whole spectrum)

$$\int\limits_0^\infty\rho^{\rm osc}(E)\,dE=\int\limits_0^\infty\rho_0(E)\,dE\,. \tag{1.15}$$

At first glance these spectral densities have completely different behavior, see Fig. 2. But we have very interesting relations between $2k\omega$-partial integral moments of this dual densities, namely, $\langle E^N\rangle_{2k\omega}\equiv\int_{2k\omega}^{2k\omega+2\omega}E^N\rho(E)\,dE$:

$$\int\limits_{2k\omega}^{2(k+1)\omega}\rho^{\rm osc}(E)\,dE\;=\;\frac{m\omega}{\pi}\;=\int\limits_{2k\omega}^{2(k+1)\omega}\rho_0(E)\,dE\,, \tag{1.16}$$

$$\int\limits_{2k\omega}^{2(k+1)\omega}E\,\rho^{\rm osc}(E)\,dE\;=\;\frac{m\omega^2(2k+1)}{\pi}\;=\int\limits_{2k\omega}^{2(k+1)\omega}E\,\rho_0(E)\,dE\,. \tag{1.17}$$

For $N\geq 2$ we have approximate relation $\langle E^N\rangle^{\rm osc}_{2k\omega}=\langle E^N\rangle^{0}_{2k\omega}\left[1+O\left(N^2/k^2\right)\right]$. So, we have duality between each excited resonance in oscillator and free particle in some spectral domain. That means *local duality*.

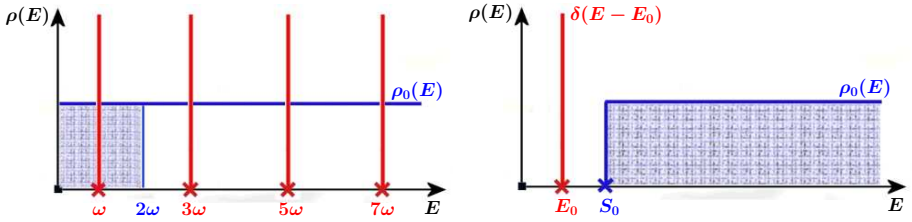


Fig. 2. Left panel: the exact spectral density $\rho^{\rm osc}(E)$ (1.13), is shown by solid vertical lines, imitating δ-functions, whereas free spectral density, $\rho_0(E)$, by the horizontal solid line. Right panel: the phenomenological model $\rho^{\rm mod}(E)$ (1.18), is shown by solid vertical line, imitating δ-function, and by the solid line, corresponding to $\rho_0(E)$ and starting from the threshold S_0.

Now we can model higher state contributions by "higher states" = "free states" outside interval $(0, S_0)$ or:

$$\rho^{\rm mod}(E) = |\psi_0(0)|^2\,\delta\,(E - E_0) + \rho_0(E)\,\theta\,(E - S_0) \tag{1.18}$$

and this gives us

$$M^{\rm mod}(\mu) = |\psi_0(0)|^2\,e^{-E_0/\mu} + \int\limits_{S_0}^{\infty}\rho_0(s)\,e^{-E/\mu}\,dE\,. \tag{1.19}$$

After all we have the following SR

$$|\psi_0(0)|^2 e^{-E_0/\mu} = \int\limits_{0}^{S_0}\rho_0(E)\,e^{-E/\mu}\,dE + \text{ power corrections}\,, \tag{1.20}$$

or, equivalently, with $\Psi_0(0) \equiv \psi_0(0)\sqrt{\pi/\omega}$:

$$|\Psi_0(0)|^2 e^{-E_0/\mu} = \frac{\mu}{2\omega}\left\{1 - e^{-S_0/\mu} - \frac{\omega^2}{6\mu^2} + \ldots\right\}\,. \tag{1.21}$$

We also have a daughter SR produced from (1.21) by applying $\partial/\partial\mu^{-1}$

$$|\Psi_0(0)|^2 E_0\,e^{-E_0/\mu} = \frac{\mu^2}{2\omega}\left\{1 - \left(1 + \frac{S_0}{\mu}\right)e^{-S_0/\mu} + \frac{\omega^2}{6\mu^2} + \ldots\right\}\,. \tag{1.22}$$

If we divide (1.22) by (1.21) we obtain SR for E_0

$$E_0 = \mu\,\frac{1 - (1 + S_0/\mu)\,e^{-S_0/\mu} + \omega^2/(6\mu^2) + \ldots}{1 - e^{-S_0/\mu} - \omega^2/(6\mu^2) + \ldots}\,. \tag{1.23}$$

The strategy of processing these SRs is:

- To determine $E_0 \approx E_0(S_0,\mu)$ by minimal sensitivity to variation of $\mu \in [\mu_{\rm L};\mu_{\rm U}]$ at appropriate S_0;
- To determine $|\Psi_0(0)|^2 \approx \Psi_0^2(S_0,E_0,\mu)$ by minimal sensitivity to variation of μ at appropriate S_0.

How we should determine the *fidelity window* $[\mu_{\rm L};\mu_{\rm U}]$? Power corrections are of the type $(\omega/\mu)^{2n}$ and they are huge at $\mu \ll \omega$. We demand:

$$\Delta_{\rm pert}(\mu) \equiv \sum_{n\geq 1} \frac{C_{2n}(\omega/\mu)^{2n}}{M_0(\mu)} \leq 0.33\,, \qquad \text{forall} \quad \mu \geq \mu_{\rm L}\,. \tag{1.24}$$

Higher states are not suppressed by $e^{-E_k/\mu} \approx 1$ at large $\mu \gg \omega$. We demand:

$$\Delta_{\rm H.S.}(\mu) \equiv \int\limits_{S_0}^{\infty} \frac{\rho_0(E)}{M_0(\mu)}\, e^{-E/\mu} dE \leq 0.33\,, \qquad \text{forall} \quad \mu \leq \mu_{\rm U}\,. \tag{1.25}$$

Then the fidelity window is $\mu_{\rm L} \leq \mu \leq \mu_{\rm U}$: Only for μ inside it is reasonable to demand minimal sensitivity of SRs to variations in μ!

Let us first consider *SR setup with fixed* E_0: We fix the energy of the ground state to the exact value, $E_0 = \omega$, and obtain the following fidelity window, $\mu_{\rm L} = 0.73\,\omega$ and $\mu_{\rm U} = 1.80\,\omega$, see Fig. 3, left panel. The result $|\Psi_0(0)|^2 = 0.99$ is obtained with only 2 power corrections included and for $S_0 = 2.08\,\omega$ (the exact value is $|\Psi_0(0)|^2 = 1$), see Fig. 3, right panel.

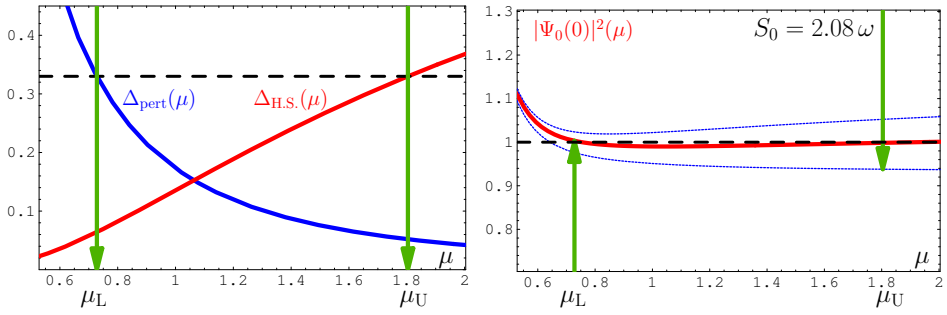


Fig. 3. Left panel: determination of the fidelity window using criteria (1.24) and (1.25). Right panel: we show here the l.h.s. of Eq. (1.21) with E_0 fixed at the exact value $E_0 = \omega$ as a function of μ. Dashed line corresponds to the position of the exact value of $|\Psi_0(0)|^2$. Positions of $\mu_{\rm L}$ and $\mu_{\rm U}$ are shown by vertical arrows in both panels and μ is displayed in units of ω.

Now we consider *SR in the complete setup*, that means that we determine the energy of the ground state from daughter SR (1.23). We take into account 3 power corrections and obtain the fidelity window $[0.74\,\omega; 1.8\,\omega]$ and $E_0 = 0.98\,\omega$ for $S_0 = 1.88\,\omega$, see Fig. 4, right panel.

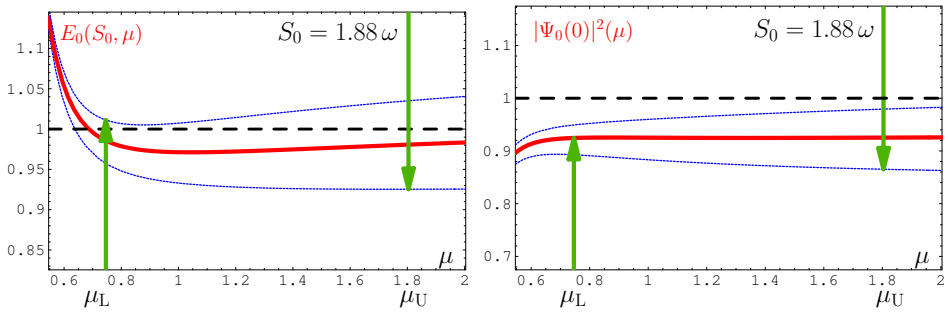


Fig. 4. Left panel: we show here the l.h.s. of Eq. (1.23), $E_0(S_0,\mu)/\omega$, as a function of μ in units of ω. Dashed line corresponds to the position of exact value of E_0. Right panel: the l.h.s. of Eq. (1.21) is shown as a function of μ in units of ω (solid line). Dashed line corresponds to the position of exact value of $|\Psi_0(0)|^2$.

Our conclusions about SRs in quantum mechanics can be summarized as follows:

- SRs give E_0 and $|\psi_0(0)|^2$ with accuracy *not worse than 10%*;
- Main source of the error — *crude model* for the spectral density of higher states: even taking into account 10 power corrections we obtain $E_0 = 0.95\,\omega$, $S_0 = 1.79\,\omega$, and $|\psi_0(0)|^2 = 0.89$;
- *But*: If we know $E_0 = 1$ exactly (say, from Particle Data Group), then accuracy can be twice higher: with taking into account 2 power corrections we obtain $S_0 = 2.08\,\omega$ and $|\psi_0(0)|^2 = 0.99$!
- In QCD spectral density more close to perturbative!

2. QCD SRs: Way to study hadrons in nonperturbative QCD

In QCD we have a big problem: nobody knows how to analyze bound states. The method of QCD SRs allows us to calculate properties of hadrons (masses, decay constants, magnetic moments) without considering hadronization or confinement issues. It was invented in 1977 by Shifman, Vainshtein & Zakharov (ITEP) [3] in order to describe J/ψ-meson, the $c\bar{c}$-system, discovered in 1974 in e^+e^--annihilation at SPEAR (SLAC) and, in parallel, in $p+$ Be collisions at BNL. In 1979 this method was applied to describe light hadrons in massless QCD [2].

Main idea: to calculate correlators of hadron currents $\langle 0|T\left[J_1(x)J_2(0)\right]|0\rangle$ by two approaches and to obtain the SR as the result of the matching. We start with the Fourier transformed correlator of two hadron currents

$$\Pi\left(Q^2\right)\mathrm{Lorentz}_{12} \equiv i\int \mathrm{e}^{iqx}\left[\langle 0|T\left[J_1(x)J_2(0)\right]|0\rangle\right]\,dx\,, \tag{2.1}$$

where $\mathrm{Lorentz}_{12}$ includes all Lorentz structures, so that $\Pi\left(Q^2\right)$ is scalar, and use the dispersion integral representation

$$\Pi(Q^2) = \int\limits_0^\infty \frac{\rho_{12}\left(s\right)\,ds}{s+Q^2} + \text{“subtractions”}\,. \tag{2.2}$$

Then we apply Borel transform defined as

$$\Phi(M^2) = \hat{B}(Q^2\to M^2)\Pi(Q^2) = \lim_{n\to\infty}\frac{(-Q^2)^n}{\Gamma(n)}\left[\frac{d^n}{dQ^{2n}}\Pi(Q^2)\right]_{Q^2=nM^2}. \tag{2.3}$$

Here we list the most important examples:

$\Pi(Q^2)$	$C=\mathrm{const}$	$C\,\log\left(Q^2/\mu^2\right)$	$1/Q^{2n}$	$1/\left(s+Q^2\right)$
$\Phi(M^2)$	0	$-C$	$1/\left(\Gamma(n)\,M^{2n}\right)$	$e^{-s/M^2}/M^2$

For us the most important are the first and the last columns in this table: we see that Borel transform kills “subtractions” and suppresses “higher states” (by the factor $\exp(-s/M^2)$ in the integrand) in (2.2):

$$B_{Q^2\to M^2}\left[\Pi(Q^2)\right] \equiv \Phi\left(M^2\right) = \int\limits_0^\infty \rho_{12}\left(s\right)\,e^{-s/M^2}\,\frac{ds}{M^2}\,. \tag{2.4}$$

In the *1-st approach* we apply the Operator Product Expansion (OPE) with account for quark and gluon condensates in QCD vacuum to obtain

$$\Phi\left(Q^2\right) = \Phi_{\mathrm{pert}}\left(Q^2\right) + c_{GG}\,\frac{\langle(\alpha_s/\pi)GG\rangle}{M^4} + c_{\bar{q}q}\,\frac{\alpha_s\langle\bar{q}q\rangle^2}{M^6}\,. \tag{2.5}$$

Here $\langle(\alpha_s/\pi)\,G^a_{\mu\nu}G^{a\mu\nu}\rangle = 0.012\,\mathrm{GeV}^4$, $\alpha_s\langle\bar{q}q\rangle^2 = 0.0018\,\mathrm{GeV}^6$ has been determined in [2] and till nowadays are practically the same [4]. The *2-nd approach* uses phenomenological saturation of spectral density by hadronic states, see (3.16),

$$\rho_{\mathrm{had}}\left(s\right) = f_h^2\delta\left(s-m_h^2\right) + \rho_{\mathrm{pert}}\left(s\right)\theta\left(s-s_0\right)\,. \tag{2.6}$$

Our model is the ground state h + continuum, which starts from threshold $s = s_0$. Then the SR is

$$f_h^2\, e^{-m_h^2/M^2} \;=\; \int\limits_0^{s_0} \rho_{\rm pert}(s)\, e^{-s/M^2}\, ds + c_{GG}\frac{\langle\frac{\alpha_s}{\pi}GG\rangle}{M^2} + c_{\bar qq}\frac{\alpha_s\langle\bar qq\rangle^2}{M^4}\,. \quad (2.7)$$

Our aim: to determine f_h^2 and m_h from this SR by calculating spectral density $\rho_{\rm pert}(s)$ and coefficients c_{GG} and $c_{\bar qq}$ and by demanding stability of this SR in variable $M^2 \in [M_L^2, M_U^2]$ with appropriate value of S_0.

3. Mesonic currents in QCD

Let us now write down the currents related to $\pi^{\pm}$-mesons in QCD:

$$\text{AV:}\quad J_{\mu 5}(x) = \bar u(x)\gamma_\mu\gamma_5 d(x)\,,\quad J^\dagger_{\mu 5}(x) = \bar d(x)\gamma_\mu\gamma_5 u(x)\,, \quad (3.1)$$

$$\text{PS:}\quad J_5(x) = i\,\bar u(x)\gamma_5 d(x)\,,\qquad J^\dagger_5(x) = i\,\bar d(x)\gamma_5 u(x)\,. \quad (3.2)$$

Note that Dirac equation $i\,\hat D\, q(x) \,=\, m_q\, q(x)$ gives us the relation:

$$\partial^\mu J_{\mu 5}(x) = (m_u + m_d)\; J_5(x)\,. \quad (3.3)$$

The decay constant f_π of the physical pion $\pi(P)$ is defined via

$$\langle 0\big|J_{\mu 5}(0)\big|\pi(P)\rangle = i\, f_\pi\, P_\mu\,. \quad (3.4)$$

It was measured in the decay $\pi \to \mu\nu_\mu$ to be $f_\pi = 132$ MeV. Eq. (3.3) then gives

$$\langle 0\big|J_5(0)\big|\pi(P)\rangle = \frac{f_\pi\, m_\pi^2}{m_u + m_d}\,, \quad (3.5)$$

meaning that the pion reveals itself both in the axial and pseudoscalar currents!

Currents related to $\rho^{\pm}$-mesons in QCD are

$$J_\mu(x) = \bar u(x)\gamma_\mu d(x)\,,\qquad J^\dagger{}_\mu(x) = \bar d(x)\gamma_\mu u(x)\,. \quad (3.6)$$

The decay constant f_ρ of physical $\rho^{\pm}(P,\varepsilon)$-meson with polarization ε and momentum P, satisfying $(P\,\varepsilon) = 0$ and $(\varepsilon,\varepsilon) = -1$, is defined through

$$\langle 0\big|J_\mu(0)\big|\rho(P,\varepsilon)\rangle = f_\rho\, m_\rho\, \varepsilon_\mu\,. \quad (3.7)$$

Decay $\rho^0 \to e^+e^-$ allows to measure $f_{\rho^0} = 150$ MeV, then from isospin symmetry we can deduce $f_{\rho^\pm} = \sqrt{2}\, f_{\rho^0} = 210$ MeV.

Interesting question: Why do we put T-product of currents in the definition (2.1) of correlators? To answer it we consider the vector current correlator $\Pi_{\mu\nu}$ in more detail. Lorentz invariance and vector current conservation dictate

$$\Pi_{\mu\nu}(q) = i \int d^4x\, e^{iqx} \langle 0 \big| T\left[J^\mu(x) J_\nu(0)\right] \big| 0\rangle = \left[q_\mu\, q_\nu - g_{\mu\nu}\, q^2\right] \Pi(q)\,. \quad (3.8)$$

Inserting $\hat{1}$ in between currents, we obtain

$$\begin{aligned} \Pi(q) \;&=\; \frac{-i\,(2\pi)^3}{3q^2} \sum_{X(p)} \delta(\vec{p}-\vec{q})\,\theta(p_0) \Big| \langle 0 \big| J_\mu(0) \big| X(p)\rangle \Big|^2 \\ &\times \int\limits_0^\infty dt\, \left[e^{i(q_0-p_0)t} + e^{-i(q_0+p_0)t} \right]. \end{aligned} \quad (3.9)$$

From Sokhotsky identity we have

$$\int\limits_0^\infty dt\, e^{\pm i\alpha t} = \pi\,\delta(\alpha) \pm i\,\mathcal{P}\frac{1}{\alpha}\,, \quad (3.10)$$

that gives us

$$\mathrm{Im}\,\Pi(q^2) = -\pi\,\frac{(2\pi)^3}{3q^2} \sum_{X(p)} \delta(\vec{p}-\vec{q})\,\delta(p_0 - |q_0|) \left| \langle 0 \big| J_\mu(0) \big| X(p)\rangle \right|^2. \quad (3.11)$$

As a result we have

$$\frac{1}{\pi}\,\mathrm{Im}\,\Pi(q^2) = \rho(q^2)\theta(|q_0|) = \rho(q^2) \quad (3.12)$$

with

$$\rho(q^2)\,\theta(q_0) = \frac{-(2\pi)^3}{3q^2} \sum_{X(p)} \delta^{(4)}(q-p)\,\theta(p_0) \Big| \langle 0 \big| J_\mu(0) \big| X(p)\rangle \Big|^2. \quad (3.13)$$

Lorentz invariance dictates that $\rho(q^2) \geq 0$. Indeed,

$$\langle 0 \big| J^\mu(x) \big| X(p)\rangle = \left[A\, p_\mu + B\, \varepsilon_\mu\right]\, e^{-ipx} \quad (3.14)$$

with $p\cdot\varepsilon = 0$, and therefore, $\varepsilon\cdot\varepsilon = -1$. From current conservation it follows $A = 0$, *i.e.* ($B = f_X\, m_X$, see (3.7))

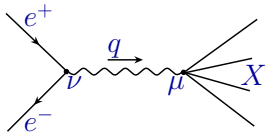
$$\langle 0 \big| J^\mu(x) \big| X(p)\rangle \langle X(p) \big| J^\dagger_\mu(x) \big| 0\rangle = \big| f_X \big|^2\, m_X^2 \varepsilon^2 = -\big| f_X \big|^2\, m_X^2 \leq 0\,. \quad (3.15)$$

This gives us

$$\rho(s) = \sum_X \left| f_X \right|^2 \delta(s - m_X^2) \geq 0\,. \tag{3.16}$$

Now we can say why we put T-product in correlators — then spectral densities, defined only by real particles, are Lorentz invariant and *depend only on* $\boldsymbol{q^2}$! Indeed, we see that the structure $e^{i(q_0-p_0)t} + e^{-i(q_0+p_0)t}$ in (3.9) appears due to the presence of the T-product in the definition of the correlator (3.8). And just this structure generates as a result $\theta(|q_0|)$ in (3.12).

Relation to the cross section of $\boldsymbol{e^+e^- \to}$ *hadrons.* We have (3.12) for the spectral density $\rho(q^2)$. This function naturally appears in 1-photon QED description of the process $e^+e^- \to$ hadrons if current J_μ is the electromagnetic current due to quarks:



$$\Leftrightarrow \quad \bar{u}(k)\gamma_\mu u(k') \frac{ie^2}{q^2} \langle X(p)|J_\mu(q)|0\rangle\,.$$

Here k and k' are the momenta of ingoing e^+ and e^-. Then we can deduce

$$\sigma_{e^+e^-\to\text{hadrons}}(s) = \frac{16\,\pi^3\,\alpha^2}{s}\,\rho(s) = \frac{4\,\pi\,\alpha^2}{3\,s}\,R(s)\,, \tag{3.17}$$

where we explicitly extracted as a factor the cross-section $\sigma_{e^+e^-\to\mu^+\mu^-}(s) = 4\,\pi\,\alpha^2/(3\,s)$ of the process $e^+e^- \to \mu^+\mu^-$. Equivalently:

$$R(s) \equiv \frac{\sigma_{e^+e^-\to\text{hadrons}}(s)}{\sigma_{e^+e^-\to\mu^+\mu^-}(s)}\,, \qquad \rho(s) = \frac{1}{12\,\pi^2}\,R(s)\,. \tag{3.18}$$

Now we can look to the quark–hadron duality, that is duality of hadron spectral density $\rho_{\text{had}}(s)$, which is measured in τ-decay to ν_τ+hadrons , and quark spectral density $\rho_{\text{pert}}(s)$ predicted by QCD:

$$\int\limits_{s_1}^{s_2} \rho_{\text{pert}}(s)\,ds = \int\limits_{s_1}^{s_2} \rho_{\text{had}}(s)\,ds\,. \tag{3.19}$$

Looking in Fig. 5 we can produce the following observations:

- Real hadron spectral density is more smooth than in QHO case;
- Duality is working!
- Asymptotics starts at $s \geq 3$ GeV^2.

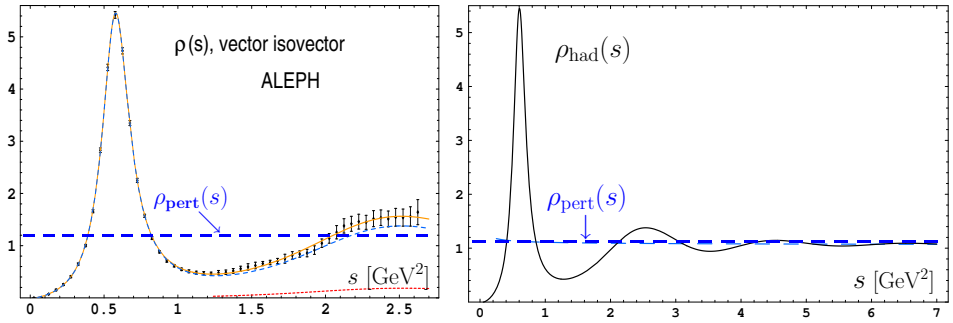


Fig. 5. We show here perturbative spectral density $4\pi^2\rho_{\rm pert}(s)$ (dashed line) in comparison with spectral density $4\pi^2\rho_{\rm had}(s)$ measured by ALEPH Collaboration.

4. Condensates in QCD

In quantum mechanics we saw that in the presence of confinement potential

$$M\left(\tau^{-1}\right) - M_0\left(\tau^{-1}\right) = \frac{m}{2\pi}\left[-\frac{1}{6}\,\omega^2\,\tau + \frac{7}{360}\,\omega^4\,\tau^3 + \dots\right].$$

This difference vanishes at short distances $\tau \ll 1/\omega$ and one can calculate exact $M(\mu)$ perturbatively, expanding in powers of the oscillator potential. In QCD *confining potential* $V^{\rm conf}(r)$ is not even known. How to proceed further? The suggestion of QCD SR approach is:

- To construct perturbative expansion in terms of quark and gluon propagators;
- To postulate that quark and gluon propagators *are modified* by the long-range confinement potential;
- To suppose that this modification is soft: at $\tau \to 0$ the difference between *exact* and *perturbative* propagators vanishes.

In realizing this program we write the exact propagator $\mathcal{S}^{\rm exact}(x,0)$ of a field ψ as a vacuum average in the exact vacuum $|0\rangle$

$$i\,\mathcal{S}^{\rm exact}(0,x) = \langle 0|\,T(\bar\psi(x)\psi(0))|0\rangle\,. \tag{4.1}$$

Wick theorem allows us to write T-product as the sum

$$T(\bar\psi(x)\psi(0)) = \bar\psi\overbrace{(x)}\psi(0) + :\bar\psi(x)\,\psi(0):\tag{4.2}$$

of the "pairing" and the "normal" product. Then

$$\mathcal{S}^{\rm exact}(0,x) = S_0(x,0) + \langle 0|:\bar\psi(x)\,\psi(0):|0\rangle\,, \tag{4.3}$$

which can be considered as the starting point to calculate power corrections in QCD. The examples in QCD are: $\langle\bar{q}q\rangle \equiv \langle 0|{:}\bar{q}(0)\,q(0){:}|0\rangle$ referred to as quark condensate; $\langle\bar{q}D^2q\rangle$, characterizing average virtuality of the vacuum quarks; gluon condensate $\langle GG\rangle \equiv \langle 0|{:}G^a_{\mu\nu}(0)\,G^a_{\mu\nu}(0){:}|0\rangle$, *etc.* Here $D_\mu \equiv \partial_\mu - igA_\mu$ is the covariant derivative and $G_{\mu\nu} = (i/g)[D_\mu, D_\nu]$ is the gluonic field strength.

Condensates and PCAC for pions in QCD. We derived the relations (3.3) and (3.4), (3.5). In order to see their consequences consider now correlator

$$\Pi_{\mu 55}(q) = i\int d^4x\, e^{iqx}\langle 0|T\left[J_{\mu 5}(x)J_5^\dagger(0)\right]|0\rangle \equiv i\,q_\mu \Pi_{\rm AP}(q^2) \qquad (4.4)$$

and its contraction with q^μ

$$\begin{aligned} i\,q^2\,\Pi_{\rm AP}(q^2) \;&=\; -\int d^3\vec{x}\,e^{-i\vec{q}\vec{x}}\left\langle 0\right|\left[J_{05}(0,\vec{x});J_5^\dagger(0)\right]\left|0\right\rangle \\ &\quad -(m_u+m_d)\int d^4x\,e^{iqx}\left\langle 0\right|T\left[J_5(x)J_5^\dagger(0)\right]\left|0\right\rangle \\ &=\; i\,\langle\bar{u}u+\bar{d}d\rangle + i\,(m_u+m_d)\,\Pi_{55}(q^2)\,. \end{aligned} \qquad (4.5)$$

Inserting pions in between currents of $\Pi_{\rm AP}(q^2)$ in (4.4) we have

$$\Pi_{\rm AP}(q^2) \approx \frac{f_\pi\, m_\pi^2}{m_u+m_d}\,\frac{f_\pi}{m_\pi^2-q^2}\Big|_{q^2\to\infty} = \frac{-f_\pi^2\, m_\pi^2}{m_u+m_d}\,\frac{1}{q^2}\left[1+O\left(\frac{m_\pi^2}{q^2}\right)\right]. \qquad (4.6)$$

Comparing asymptotics $O(1/q^2)$ of (4.5) and (4.6) gives us the famous *PCAC relation*:

$$f_\pi^2\, m_\pi^2 \;=\; -\langle\bar{u}u+\bar{d}d\rangle\,(m_u+m_d) + O\left(m_q^2\right)\,. \qquad (4.7)$$

In fact we should add other possible PS-meson states to obtain

$$f_\pi^2\, m_\pi^2 + f_{\pi'}^2\, m_{\pi'}^2 + \ldots \;=\; -\langle\bar{u}u+\bar{d}d\rangle\,(m_u+m_d) + O\left(m_q^2\right)\,. \qquad (4.8)$$

In the chiral limit, $m_q \to 0$, PCAC relation tells us:

- $f_\pi \neq 0$, then $m_\pi \to 0 \Rightarrow$ pion is Goldstone boson;
- $m_{\pi'} \neq 0$, then $f_{\pi'} \to 0 \Rightarrow$ no decays $\pi' \to \mu\nu_\mu$!
- $m_\pi \approx f_\pi \approx 130$ MeV $\Rightarrow \langle\bar{q}q\rangle \approx -(260\ \text{MeV})^3$ at $m_u = m_d = 4$ MeV.

5. QCD SRs for π-mesons

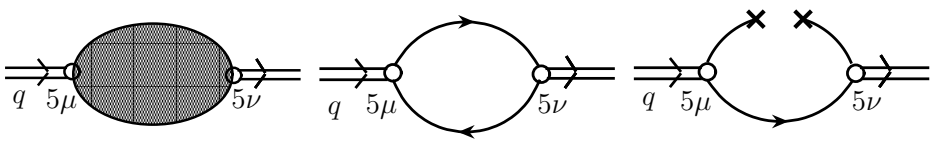
We study axial-axial correlator $\Pi_{\mu 5;\nu 5}(q)$

$$i\int d^4x\, e^{iqx}\left\langle 0\Big|T\left[J_{\mu 5}(x)J^{\dagger}_{\nu 5}(0)\right]\Big|0\right\rangle \equiv g_{\mu\nu}\Pi_1(q^2)+q_\mu q_\nu \Pi_2(q^2)\,.$$

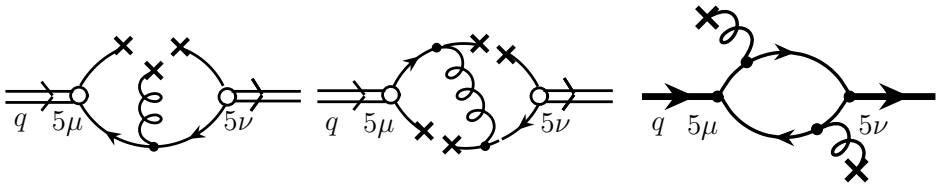
Hadronic contribution to Borel transform of $\Pi_2(q^2)$:

$$\Phi^{\rm hadr}\left(M^2\right)=B_{Q^2\to M^2}\left[\Pi_2^{\rm hadr}(q^2)\right]=\frac{f_\pi^2}{M^2}+\frac{f_{A_1}^2}{M^2}\,e^{-m_{A_1}^2/M^2}+\ldots\,.$$

The following diagrams contributes to the OPE of this correlator



$$\Phi_{\rm OPE}\left(M^2\right) \quad = \quad \Phi_{\rm pert}\left(M^2\right) \quad + \quad \Phi_{\rm 2V}\left(M^2\right)$$



$$+ \quad \Phi_{\rm 3L}\left(M^2\right) \quad + \quad \Phi_{\rm 4Q}\left(M^2\right) \quad + \quad \Phi_{\rm GG}\left(M^2\right)$$

with $\Phi_{\{\rm 2V,3L,4Q\}}(M^2)=\{16,16,144\}\,(\pi\alpha_s\langle\bar qq\rangle^2)/(81\,M^6)$. We see that in the quark condensate contribution the most important one is $\Phi_{\rm 4Q}$. As a result we have the following SR for the pion decay constant

$$f_\pi^2=\frac{M^2}{4\pi^2}\left(1-e^{-s_0/M^2}\right)\left[1+\frac{\alpha_s}{\pi}\right]+\frac{1}{12\,\pi}\,\frac{\langle\alpha_s\,GG\rangle}{M^2}+\frac{176}{81}\,\frac{\pi\alpha_s\langle\bar qq\rangle^2}{M^4}\,. \quad (5.1)$$

Numerically, as can be seen from Fig. 6, we obtain $f_\pi=0.128\pm0.13$ GeV from this SR, whereas in the spectral model with A_1-meson we obtain slightly higher value $f_\pi=0.137\pm0.13$ GeV, to be compared with $f_\pi^{\rm exp}=0.132$ GeV.

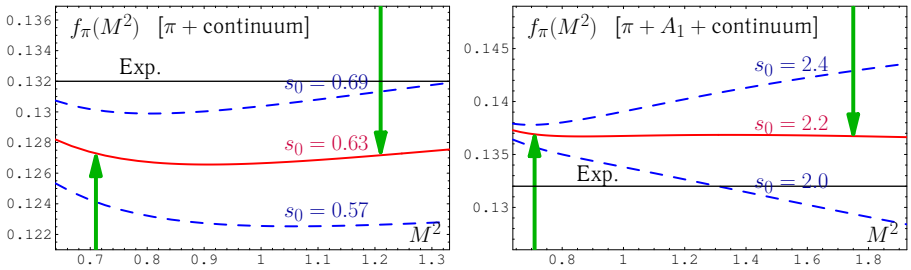


Fig. 6. Left panel: we show here the l.h.s. of Eq. (5.1), $f_\pi^2(M^2)$, as a function of M^2 (solid line). Right panel: the same as in the left panel, but for the spectral model $\pi + A_1 + \text{continuum}$. Dashed lines correspond to 10% variations of the best thresholds. Positions of M_{L}^2 and M_{U}^2 are shown by vertical arrows in both panels.

6. Generalized QCD SRs for mesonic distribution amplitudes

The *pion distribution amplitude* (DA) parameterizes the matrix element of the nonlocal axial current on the light cone [5]

$$\langle 0\,|\,\bar{d}(z)\gamma_\mu\gamma_5 E(z,0)u(0)\,|\,\pi(P)\rangle\Big|_{z^2=0} = if_\pi P_\mu \int\limits_0^1 dx\; e^{ix(zP)}\varphi_\pi^{\text{Tw-2}}(x,\mu^2)\,. \quad (6.1)$$

Here the gauge-invariance is guaranteed by the Fock–Schwinger string

$$E(z,0) = \mathcal{P}\exp\left[ig\int\limits_0^z A_\mu(\tau)d\tau^\mu\right]$$

in between separated quark fields. The physical meaning of this DA — the amplitude of the transition $\pi(P) \to u(Px) + \bar{d}(P(1-x))$. It is convenient to represent the pion DA:

$$\varphi_\pi(x;\mu^2) = \varphi^{\text{As}}(x)\left[1 + \sum_{n\geq 1} a_{2n}(\mu^2)\, C_{2n}^{3/2}(2x-1)\right], \quad (6.2)$$

where $C_n^{3/2}(2x-1)$ are the Gegenbauer polynomials (1-loop eigenfunctions of ER-BL kernel) and $\varphi^{\text{As}}(x) = 6\,x\,(1-x)$. This representations means that all scale dependence in $\varphi_\pi(x;\mu^2)$ is transformed to the scale dependence of the set $\{a_2(\mu^2), a_4(\mu^2), \ldots\}$. ER-BL solution at the 2-loop level is also possible with using the same representation (6.2) [6–9].

In order to construct reliable SRs for the pion DA moments one needs, as has been shown in [10, 11], to take into account the *nonlocality of QCD*

vacuum condensates. For an illustration of the nonlocal condensate (NLC) model we use here the minimal Gaussian model

$$\langle \bar{q}(0) q(z) \rangle = \langle \bar{q}\, q \rangle\, e^{-|z^2|\lambda_q^2/8}\,. \tag{6.3}$$

The single scale parameter $\lambda_q^2 = \langle k^2 \rangle$ characterizes the average momentum of quarks in the QCD vacuum and has been estimated in QCD SR approach and also on the lattice [12–16]:

$$\lambda_q^2 = 0.35 - 0.55 \text{ GeV}^2\,. \tag{6.4}$$

That means that λ_q^2 is of an order of the typical hadronic scale $m_\rho^2 \approx 0.6\,\text{GeV}^2$. We write down as an example the NLC QCD SR for the pion DA itself. To produce it one starts with a correlator of currents $J_{\mu 5}(x)$ and $J^\dagger_{\nu 5;N}(0) = \bar{d}(0)\,\hat{n}\,\gamma_5\,(n\nabla)^N u(0)$ with light-like vector n, $n^2 = 0$, obtains SRs for the moments $\langle x^N \rangle_\pi$ and then realizes inverse Mellin transform from the moments $\langle x^N \rangle_\pi$ to the DA $\varphi_\pi(x)$:

$$\begin{aligned} f_\pi^2\, \varphi_\pi(x) \;=\; & \int\limits_0^{s_{\pi 0}} \rho^{\text{pert}}(x;s)\, e^{-s/M^2}\, ds + \frac{\langle (\alpha_s/\pi) GG \rangle}{24 M^2}\, \varphi_{GG}(x;\Delta) \\ & + \frac{8\pi\alpha_s \langle \bar{q} q \rangle^2}{81 M^4} \sum_{i=2V,3L,4Q} \varphi_i(x;\Delta)\,. \end{aligned} \tag{6.5}$$

The local limit $\lambda_q^2/M^2 \equiv \Delta \to 0$ of this SR is specified by the appearance of δ-functions concentrated at the end-points $x = 0$ and $x = 1$, for example, $\varphi_{GG}(x;\Delta) = [\delta(x) + \delta(1-x)]$ and $\varphi_{4Q}(x;\Delta) = 9[\delta(x) + \delta(1-x)]$. The minimal Gaussian model (6.3) generates the contribution $\varphi_{4\text{Q}}(x;\Delta)$ shown in the left panel of Fig. 7 in comparison with perturbative one for the standard (local) and the NLC types of the SR. We see that in the local version due to completely different behavior of perturbative and condensate terms it is difficult to obtain some kind of consistency. Alternatively, the NLC contribution is much more similar to the perturbative one — and for this reason in the NLC SR we have a very good stability! After processing the SR (6.5) for the moments (at $\mu^2 \simeq 1.35\,\text{GeV}^2$)

$$\left\langle \xi^N \right\rangle_\pi = \int\limits_0^1 \varphi_\pi(x)\; (2x-1)^N\, dx\,, \tag{6.6}$$

we restore the pion DA $\varphi_\pi(x)$ by demanding that it should reproduce these 5 moments and applying the minimally possible number of the Gegenbauer

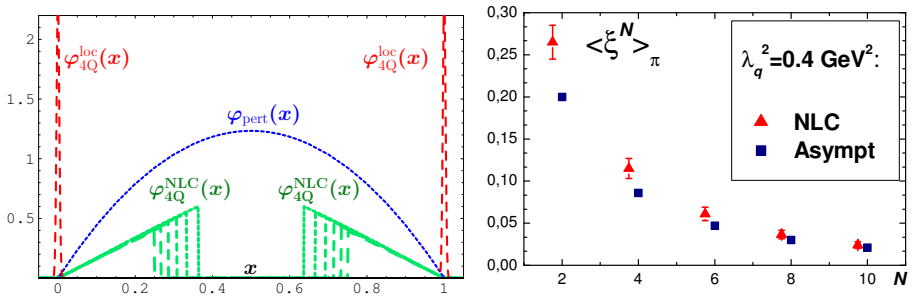


Fig. 7. Left panel: we show here contributions to the r.h.s. of Eq. (6.5) due to perturbative loop (dotted line) and due to 4Q-condensate: $\varphi^{\rm loc}_{\rm 4Q}(x)$ — in standard QCD SRs, and $\varphi^{\rm NLC}_{\rm 4Q}(x, M^2)$ (with $M^2 = 0.55 - 0.80\,{\rm GeV}^2$) — in NLC QCD SRs. Right panel: moments $\langle \xi^{2N} \rangle_\pi$ with $N = 1, \ldots, 5$, obtained using the NLC SR (6.5), are shown by triangles with error-bars. We show also for comparison the asymptotic DA moments (squares).

harmonics in representation (6.2). It appears the NLC SRs for the pion DA produce a bunch of *self-consistent 2-parameter models* at $\mu^2 \simeq 1.35\,{\rm GeV}^2$

$$\varphi^{\rm NLC}_\pi(x;\mu^2) = \varphi^{\rm As}(x)\left[1 + \sum_{n=1,2} a_{2n}(\mu^2)\, C^{3/2}_{2n}(2x-1)\right]. \qquad (6.7)$$

The central point corresponds to $a_2^{\rm BMS} = +0.188$, $a_4^{\rm BMS} = -0.130$ in the case $\lambda_q^2 = 0.4$ GeV^2, whereas other allowed values of parameters a_2 and a_4 are shown in the left panel of Fig. 8 as the gray slanted rectangle [17].

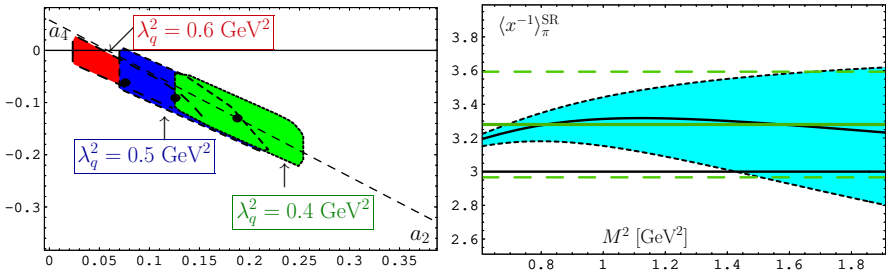


Fig. 8. Left panel: the allowed values of parameters a_2 and a_4 of the bunches (6.7) at $\mu^2 = 1.35\,{\rm GeV}^2$ for three values of the nonlocality parameter λ_q^2: $0.4\,{\rm GeV}^2$ (gray region), $0.5\,{\rm GeV}^2$ (black region), and $0.6\,{\rm GeV}^2$ (dark gray region). Right panel: the inverse moment $\langle x^{-1} \rangle_\pi$, obtained using the NLC SR (6.5), is shown by the solid line (central value) with error-bars, shown as dashed lines.

We verify that this solution is self-consistent by estimating the inverse moment of the pion DA, $\langle x^{-1}\rangle_\pi$, in two ways. The first is based on (6.7) and gives us

$$\langle x^{-1}\rangle_\pi^{\rm bunch} = 3.17 \pm 0.20\,. \tag{6.8}$$

The second way uses the special SR for this moment, obtained through the basic SR (6.5). It is worth to emphasize here that the moment $\langle x^{-1}\rangle_\pi^{\rm SR}$ could be determined only in NLC SRs because the end-point singularities absent. This SR produces the estimate, see Fig. 8, right panel:

$$\langle x^{-1}\rangle^{\rm SR} = 3.30 \pm 0.30 \tag{6.9}$$

at $\mu^2 \simeq 1.35\,{\rm GeV}^2$. We see that both estimates are in a good agreement.

Comparing the obtained pion DA with the Chernyak&Zhitnitsky (CZ) one [18], see Fig. 9, reveals that although both DAs are two-humped they are quite different: our DA is strongly end-point suppressed. This can also be verified in the right panel of the figure, where contributions of different bins to inverse moment $\langle x^{-1}\rangle_\pi$, calculated as $\int_x^{x+0.02}\phi(x)dx$ and normalized to 100%, are shown for CZ and BMS DAs.

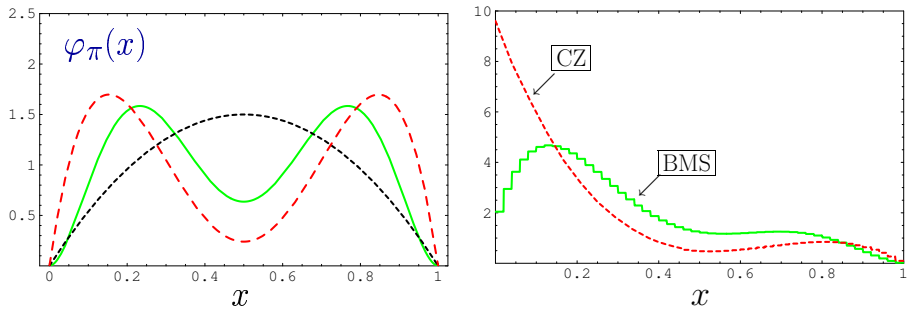
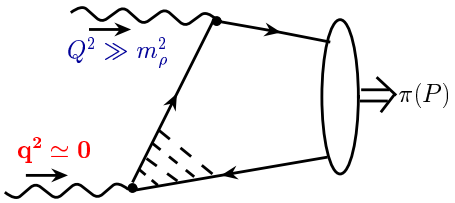


Fig. 9. Left panel: we show here the comparison of curves for three DAs — BMS (solid line), CZ (dashed line), and the asymptotic DA (dotted line). Right panel: histograms for contributions of different bins to inverse moment $\langle x^{-1}\rangle_\pi$ are shown for CZ and BMS DAs.

7. LCSR analysis of CLEO data on $F_{\gamma\gamma^*\pi}(Q^2)$ and pion DA

Why does one need to use Light-Cone SRs (LCSRs) in analyzing the experimental data on $\gamma^*(Q)\gamma(q) \to \pi^0$-transition form factor? For $Q^2 \gg m_\rho^2$, $q^2 \ll m_\rho^2$ the QCD factorization is valid only in the leading twist approximation and the higher twists are of importance [19]. The reason is evident: if $q^2 \to 0$ one needs to take into account interaction of a real photon at

long distances of order of $O(1/\sqrt{q^2})$. To account for long-distance effects in perturbative QCD one needs to introduce the light-cone DA of the real photon.



Instead of doing so, Khodjamirian [20] suggested to use the LCSR approach, which effectively accounts for long-distances effects of the real photon using the quark–hadron duality in the vector channel and dispersion relation in q^2.

We refined the NLO analysis of the CLEO data [21] by taking into account the following items:

(i) an accurate NLO evolution for both $\varphi(x, Q^2_{\rm exp})$ and $\alpha_s(Q^2_{\rm exp})$ with accounting for quark thresholds;

(ii) the relation between the "nonlocality" scale and the twist-4 magnitude $\delta^2_{\rm Tw\text{-}4} \approx \lambda_q^2/2$ was used to re-estimate $\delta^2_{\rm Tw\text{-}4} = 0.19 \pm 0.02$ at $\lambda_q^2 = 0.4\,{\rm GeV}^2$;

(iii) the possibility to extract constraints on $\langle x^{-1}\rangle_\pi$ from the CLEO data and to compare them with what we have from NLC QCD SRs.

The results of our analysis [22] are displayed in Fig. 10. Solid lines in all figures enclose the 2σ-contours, whereas the 1σ-contours are enclosed by dashed lines. The three slanted and shaded rectangles represent the

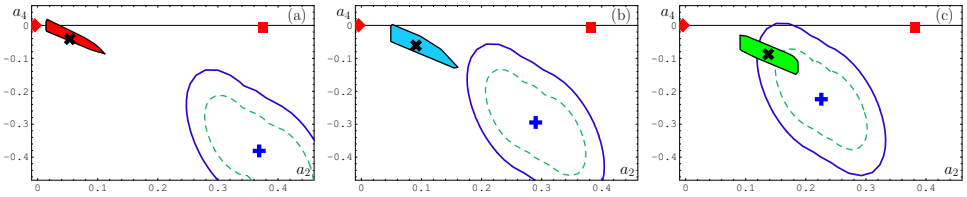


Fig. 10. Three 2σ-contours of the admissible regions following from the analysis of the CLEO data for different values of δ^2: (a) for $\lambda_q^2 = 0.6\,{\rm GeV}^2$ and $\delta^2_{\rm Tw\text{-}4} = (0.29 \pm 0.03)\,{\rm GeV}^2$; (b) for $\lambda_q^2 = 0.5\,{\rm GeV}^2$ and $\delta^2_{\rm Tw\text{-}4} = (0.235 \pm 0.025)\,{\rm GeV}^2$; (c) for $\lambda_q^2 = 0.4\,{\rm GeV}^2$ and $\delta^2_{\rm Tw\text{-}4} = (0.19 \pm 0.02)\,{\rm GeV}^2$.

constraints on $(a_2,\ a_4)$ posed by the QCD SRs [17] for corresponding values of $\lambda_q^2 = 0.4,\ 0.5,\ 0.6\,\mathrm{GeV}^2$ (from left to right). All values are evaluated at $\mu^2 = 2.4\ \mathrm{GeV}^2$ after the NLO evolution.

We see that the CLEO data definitely prefer the value of the QCD nonlocality parameter $\lambda_q^2 = 0.4\,\mathrm{GeV}^2$. We also see in Fig. 10(c) (and this conclusion was confirmed even with 20% uncertainty in twist-4 magnitude, see also Fig. 11) that CZ DA (■) is excluded at least at 4σ-level, whereas the asymptotic DA (◆) — at 3σ-level. In the same time our DA (✖) and most of the bunch (the slanted shaded rectangle around the symbol ✖) are inside 1σ-domain. Instanton-based models are all near 3σ-boundary and only the Krakow model [23], denoted in Fig. 11 by symbol ✦, is close to 2σ-boundary. In the left panel of Fig. 11 we demonstrate the 1σ, 2σ and 3σ-contours (solid, dotted and dashed contours around the best-fit point (✚)), which have been obtained for values of the twist-4 scale parameter $\delta^2_{\text{Tw-4}} = [0.15\text{–}0.23]\,\mathrm{GeV}^2$. As one sees from the straight dashed line within the hatched band, corresponding in this figure to the mean value of $\langle x^{-1}\rangle_\pi^{\mathrm{SR}}/3 - 1$ and its error bars, the nonlocal QCD sum-rules result with its error bars appears to be in good agreement with the CLEO-constraints on $\langle x^{-1}\rangle_\pi^{\mathrm{exp}}$ at the 1σ-level. Moreover, the estimate $\langle x^{-1}\rangle_\pi^{\mathrm{SR}}$ is close to $\langle x^{-1}\rangle_\pi^{\mathrm{EM}}/3 - 1 = 0.24 \pm 0.16$, obtained in the data analysis of the electromagnetic pion form factor within the framework of a different LCSR method in [24, 25]. These three independent estimates are in good agreement to each other, giving firm support that the CLEO data processing, on one hand, and the theoretical calculations, on the other, are mutually consistent.

Another possibility, suggested in [26], to obtain constraints on the pion DA in the LCSR analysis of the CLEO data — to use for the twist-4 contribution renormalon-based model, relating it then to parameters a_2 and

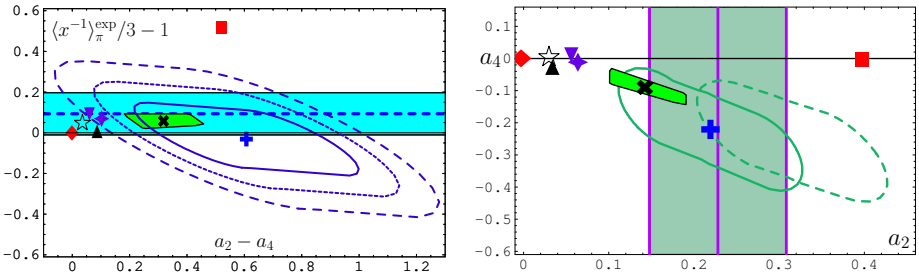


Fig. 11. The results of the CLEO data analysis for the pion DA parameters ($\langle x^{-1}\rangle_\pi^{\mathrm{exp}}/3 - 1$, evaluated at $\mu_0^2 \approx 1\ \mathrm{GeV}^2$, in the left panel, and a_2 and a_4, evaluated at $\mu^2_{\mathrm{SY}} = 5.76\,\mathrm{GeV}^2$ — in the right panel). In the right panel the lattice results of [29] are shown for comparison as shaded area, whereas the renormalon-based 1σ-ellipse of [27] is displayed by the dashed line.

a_4 of the pion DA. Using this method we obtain [27] the renormalon-based constraints for the parameters a_2 and a_4, shown in the right panel of Fig. 11 in a form of 1σ-ellipses (dashed contour).

New high-precision lattice measurements of the pion DA second moment $\langle\xi^2\rangle_\pi = \int_0^1 (2x-1)^2 \varphi_\pi(x)\, dx$ appeared rather recently [28, 29]. Both groups extracted from their respective simulations, values of a_2 at the Schmedding–Yakovlev scale $\mu^2_{\rm SY}$ around 0.24, but with different error bars.

It is remarkable that these lattice results are in striking agreement with the estimates of a_2 both from NLC QCD SRs [17] and also from the CLEO-data analyses — based on LCSR — [21, 22], as illustrated in the right panel of Fig. 11, where the lattice results of [29] are shown in the form of a vertical strip, containing the central value with associated errors being smaller than in [28]. Noteworthily, the value of a_2 of the displayed lattice measurements (middle line of the strip) is very close to the CLEO best fit in [22] (✚).

8. Pion form factor and CEBAF data

It is worth to mention here the results of our analysis of the pion electromagnetic form factor using NLC dictated pion DA and Analytic Perturbative QCD [30]. These results are in excellent agreement with CEBAF data on pion form factor, shown as diamonds in Fig. 12, where the green strip includes both the NLC QCD SRs uncertainties, generated by our bunch of the allowed pion DA, and by the scale-setting ambiguities at the NLO level.

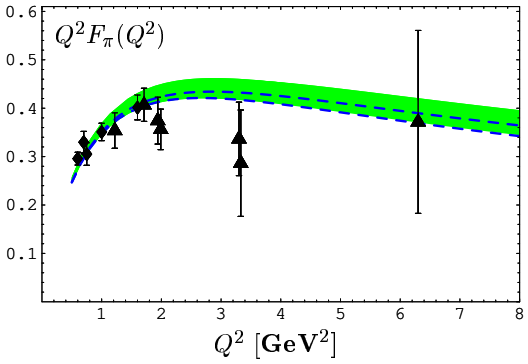


Fig. 12. Predictions for the scaled pion form factor calculated with the BMS bunch (gray strip) encompassing nonperturbative uncertainties from nonlocal QCD sum rules [17] and renormalization scheme and scale ambiguities at the level of the NLO accuracy. The dashed lines inside the strip indicate the corresponding area of predictions obtained with the asymptotic pion DA. The experimental data are taken from [31] (diamonds) and [32], [33] (triangles).

From the phenomenological point of view, the most interesting result here is that the BMS pion DA [17] (out of a "bunch" of similar doubly-peaked endpoint-suppressed pion DAs) yields to predictions for the electromagnetic form factor very close to those obtained with the asymptotic pion DA. Conversely, we see that a small deviation of the prediction for the pion form factor from that obtained with the asymptotic pion DA does not necessarily imply that the underlying pion DA has to be close to the asymptotic profile. Much more important is the behavior of the pion DA in the endpoint region $x \to 0\,, 1$.

9. Conclusions

Let me conclude with the following observations:

- NLC QCD SR method for the pion DA gives us the admissible bunches of DAs for each value of λ_q.
- NLO LCSR method produces new constraints on the pion DA parameters (a_2 and a_4) in conjunction with the CLEO data.
- Comparing results of the NLC SRs with new CLEO constraints allows to fix the value of QCD vacuum nonlocality: $\lambda_q^2 \simeq 0.4\,\mathrm{GeV}^2$.
- This bunch of pion DAs agrees well with recent lattice data and with JLab F(pi) data on the pion form factor.

I also suggest to the reader to look in the very interesting discussion of the QCD SR approach and its developments written by one of its creators [34].

This investigation was supported in part by the Bogoliubov–Infeld Programme, grant 2006, by the Heisenberg–Landau Programme, grant 2006, and the Russian Foundation for Fundamental Research, grant No. 06-02-16215.

REFERENCES

[1] A.V. Radyushkin, Proceedings of the 13th Annual HUGS AT CEBAF (HUGS 98), 26 May–2 Jun 1998, Newport News, Virginia, edited by J.L. Goity, World Scientific, Singapore 2000, pp. 91–150.

[2] M.A. Shifman, A.I. Vainshtein, V.I. Zakharov, *Nucl. Phys.* **B147**, 385 (1979); *Nucl. Phys.* **B147**, 448 (1979); *Nucl. Phys.* **B147**, 519 (1979).

[3] V.A. Novikov, *et al., Phys. Rep.* **41**, 1 (1978).

[4] B.L. Ioffe, K.N. Zyablyuk, *Nucl. Phys.* **A687**, 437 (2001); B.V. Geshkenbein, B.L. Ioffe, K.N. Zyablyuk, *Phys. Rev.* **D64**, 093009 (2001).

[5] A.V. Radyushkin, Dubna preprint P2-10717, 1977 [hep-ph/0410276].

[6] S.V. Mikhailov, A.V. Radyushkin, *Nucl. Phys.* **B273**, 297 (1986).

[7] E.P. Kadantseva, S.V. Mikhailov, A.V. Radyushkin, *Sov. J. Nucl. Phys.* **44**, 326 (1986).

[8] D. Müller, *Phys. Rev.* **D49**, 2525 (1994); *Phys. Rev.* **D51**, 3855 (1995).

[9] A.P. Bakulev, N.G. Stefanis, *Nucl. Phys.* **B721**, 50 (2005).

[10] S.V. Mikhailov, A.V. Radyushkin, *JETP Lett.* **43**, 712 (1986); *Sov. J. Nucl. Phys.* **49**, 494 (1989); *Phys. Rev.* **D45**, 1754 (1992).

[11] A.P. Bakulev, S.V. Mikhailov, *Phys. Lett.* **B436**, 351 (1998).

[12] V.M. Belyaev, B.L. Ioffe, *ZhETF* **83**, 876 (1982).

[13] A.A. Ovchinnikov, A.A. Pivovarov, *Sov. J. Nucl. Phys.* **48**, 721 (1988).

[14] A.A. Pivovarov, *Bull. Lebedev Phys. Inst.* **5**, 1 (1991).

[15] M. D'Elia, A. Di Giacomo, E. Meggiolaro, *Phys. Rev.* **D59**, 054503 (1999).

[16] A.P. Bakulev, S.V. Mikhailov, *Phys. Rev.* **D65**, 114511 (2002).

[17] A.P. Bakulev, S.V. Mikhailov, N.G. Stefanis, *Phys. Lett.* **B508**, 279 (2001); Proceedings of the 36th Rencontres De Moriond On QCD And Hadronic Interactions, 17–24 Mar 2001, Les Arcs, France, ed. by J.T.T. Van, World Scientific, Singapore 2002, pp. 133–136.

[18] V.L. Chernyak, A.R. Zhitnitsky, *Nucl. Phys.* **B201**, 492 (1982); *Nucl. Phys.* **B214**, 547(E) (1983).

[19] A.V. Radyushkin, R. Ruskov, *Nucl. Phys.* **B481**, 625 (1996).

[20] A. Khodjamirian, *Eur. Phys. J.* **C6**, 477 (1999).

[21] A. Schmedding, O. Yakovlev, *Phys. Rev.* **D62**, 116002 (2000).

[22] A.P. Bakulev, S.V. Mikhailov, N.G. Stefanis, *Phys. Rev.* **D67**, 074012 (2003); *Phys. Lett.* **B578**, 91 (2004).

[23] M. Praszalowicz, A. Rostworowski, *Phys. Rev.* **D64**, 074003 (2001).

[24] V.M. Braun, A. Khodjamirian, M. Maul, *Phys. Rev.* **D61**, 073004(2000).

[25] J. Bijnens, A. Khodjamirian, *Eur. Phys. J.* **C26**, 67 (2002).

[26] S.S. Agaev, *Phys. Rev.* **D72**, 114010 (2005).

[27] A.P. Bakulev, S.V. Mikhailov, N.G. Stefanis, *Phys. Rev.* **D73**, 056002 (2006).

[28] L. Del Debbio, *Few Body Syst.* **36**, 77 (2005).

[29] M. Göckeler *et al.*, talk in the Workshop on Light-Cone QCD and Nonperturbative Hadron Physics 2005 (LC 2005), Cairns, Queensland, Australia, 7–15 Jul 2005 [`hep-lat/0510089`].

[30] A.P. Bakulev *et al.*, *Phys. Rev.* **D70**, 033014 (2004).

[31] J. Volmer *et al.*, *Phys. Rev. Lett.* **86**, 1713 (2001).

[32] C.N. Brown *et al.*, *Phys. Rev.* **D8**, 92 (1973).

[33] C.J. Bebek *et al.*, *Phys. Rev.* **D13**, 25 (1976).

[34] M. Shifman, `hep-ph/9802214`.